FEBS Letters 512 (2002) 298–302 FEBS 25751

Three-dimensional architecture of the eukaryotic multisynthetase complex determined from negatively stained and cryoelectron micrographs

Mona T. Norcum[a,*], Nicolas Boisset[b]

[a] *Department of Biochemistry, The University of Mississippi Medical Center, 2500 North State Street, Jackson, MS 39216, USA*
[b] *Laboratoire de Minéralogie Cristallographie, Universités Paris 6 et Paris 7, Paris Cedex 05, France*

Received 7 December 2001; revised 23 December 2001; accepted 24 December 2001

First published online 24 January 2002

Edited by Lev Kisselev

Abstract This study provides the first description of the three-dimensional architecture of the multienzyme complex of aminoacyl-tRNA synthetases. Reconstructions were calculated from electron microscopic images of negatively stained and frozen hydrated samples using three independent angular assignment methods. In all cases, volumes show an asymmetric triangular arrangement of protein domains around a deep central cavity. The structures have openings or indentations on most sides. Maximum dimensions are ca. 19×16×10 nm. The central cavity is 4 nm in diameter and extends two-thirds of the length of the particle. © **2002 Published by Elsevier Science B.V. on behalf of the Federation of European Biochemical Societies.**

Key words: Aminoacyl-tRNA synthetase; Multisynthetase complex; Electron microscopy; Three-dimensional reconstruction

1. Introduction

The aminoacyl-tRNA synthetase family has long been of biochemical significance and interest because of the essential role of these proteins in proper pairing of amino acids with tRNAs prior to protein biosynthesis. Because of the large number of proteins in this family, much information has been obtained, especially in prokaryotes, about their individual structures, enzymatic mechanisms, and evolution (reviewed in [1]). Recently, additional excitement has been generated by demonstration of alternative functions of these enzymes, such as proofreading of tRNAs prior to nuclear export, RNA splicing, as well as their association with precursors of inflammatory cytokines and potential as new targets for antimicrobial agents (reviewed in [2]).

A subset of aminoacyl-tRNA synthetases is isolated from multicellular eukaryotes as a multienzyme complex. Regardless of cell or tissue type, this particle contains nine aminoacyl-tRNA synthetases. These are the enzymes for arginine, aspartic acid, glutamine, isoleucine, leucine, lysine, methionine, as well as the bifunctional polypeptide containing the activities for glutamine and proline. There are three additional proteins in the ca. 1×10^6 Da complex: p18, p38, and p43. This last polypeptide has been the subject of intense study because it is the precursor form [3] of the inflammatory cytokine endothelial-monocyte activating polypeptide II (EMAPII). Although the biochemistry of the multisynthetase complex has been studied for many years (reviewed in [4]), it is only recently that we have developed a working model of the particle based on structural information [5]. In this model, the multisynthetase complex is composed of three domains arranged in a Y-shape and includes specific locations for enzymes within the domains. Immunoelectron microscopic localizations of the glutamyl/prolyl-tRNA synthetase and of p43 (pro-EMAPII) within the complex [6,7], as well as two-hybrid analyses [8,9], are consistent with the model and have aided in its refinement.

However, the three-dimensional structure of the multisynthetase complex is essential for determination of the exact distribution of proteins within the particle, definition of the arrangement of enzyme active sites, and characterization of the structural and functional relationships between the well known cytosolic particle and the recently reported nuclear [10] version. This study presents the first such information determined by computational microscopy for the rabbit reticulocyte multisynthetase complex. Volumes were calculated from images of negatively stained and frozen hydrated samples. Moreover, three different methods of angular assignment were used to assure that the calculations provided accurate structural representations.

2. Materials and methods

2.1. Protein purification

The multisynthetase complex was isolated from rabbit reticulocyte lysate (Green Hectares) as described previously [5].

2.2. Electron microscopy

Samples were diluted to 15 or 20 μg/ml in 25 mM HEPES, pH 7.2, 100 mM NaCl then stabilized with 0.3% glutaraldehyde [11]. Negatively stained preparations were embedded in a deep layer of uranyl acetate on a thick carbon film. First, the carbon films were made hydrophilic by applying 5 μl of 0.1% (w/v) polylysine (Polysciences) to the carbon-coated grid (Polysciences). This was wicked off and 5 μl of sample immediately added. After 1 min, the grid was washed with three drops of 1% (w/v) uranyl acetate. Most of the large drop of stain remaining on the grid was wicked away by touching the edge to filter paper and then the grid was air-dried. After microdialysis to remove excess glycerol [12], frozen hydrated samples were prepared by plunging into liquid ethane [13]. Image pairs were collected with the sample grid tilted (45° or 50°) or untilted (0°). Images were taken with mini-

*Corresponding author. Fax: (1)-601-984 1855.
E-mail addresses: mnorcum@biochem.umsmed.edu (M.T. Norcum), nicolas.boisset@imcp.jussieu.fr (N. Boisset).

0014-5793/02/$22.00
PII: S0014-5793(02)02262-7

mum dose focusing on LEO 912 electron microscopes at absolute magnifications of 50 000 or 45 000. Estimated electron dose for all data sets was 20 electrons/Å^2 or less. Flatbed scanners were used for digitization at resolutions of 4.06 or 4.51 Å/pixel on the image scale.

2.3. Image analysis

Computations were done using SPIDER software [14]. The random conical tilt reconstruction scheme was applied to the negatively stained data set [15]. Briefly, images were interactively selected, aligned using a reference-free method [16], then further aligned and classified using a K-means splitting algorithm [17]. Three-dimensional structures of appropriate class averages were calculated by iterative back projection from the tilted-specimen images. Forty-two three-dimensional structures were calculated from class averages. Each volume was compared to the others by three-dimensional alignment [16] then merged volumes were calculated using the Eulerian angles which gave cross-correlation coefficients of 0.87 or greater. The process was repeated five times until an isotropic reference volume was obtained. Untilted-specimen images were aligned to projections of this volume and were used for six rounds of iterative back projection to produce refined structures. For frozen hydrated samples, two methods of reconstruction were used using untilted images. First, after reference-free alignment and classification as above, the reconstruction angles were determined by projection mapping to the reference volume calculated from the negatively stained images. Second, an orientation search method [17] was applied to the averages resulting from reference-free alignment and classification.

Resolution limits were determined from the 50 percent cutoff of Fourier shell correlation between volumes calculated from half data sets. The threshold for surface display of the negatively stained volume was determined by calculating the voxels required for 100% of the molecular mass. Relying on a voxel size of $4\times4\times4$ Å^3, a total mass of 1.1×10^6 Da as calculated using accepted polypeptide stoichiometries [4] and a partial specific volume of 0.73 cm^3/g, the estimated volume occupied by the complex should be approximately 1330 cm^3. This value provides an absolute scale for future comparisons and the surface representations presented in this study delineate this expected volume.

2.4. Image presentation

IRIS Explorer (Numerical Algorithms Group) was used for surface representations of the volumes in Fig. 2. All other visualizations were done with the WEB component of SPIDER. Composites were constructed using Showcase and Snapshot (Silicon Graphics).

3. Results

3.1. Consistency of electron microscopic images

In previous studies, electron microscopic images of the multisynthetase complex were obtained using negatively stained samples prepared by a 'double carbon' method [11] from which characteristic views were identified. The most distinctive of these were described as a 'cup' or broad V-shape with a central cleft, a triangle and rectangle. In the present study, possible particle distortion or flattening was obviated by adsorption of the samples to a single carbon layer followed by embedding in a thick layer of stain. Fig. 1 shows that this technique provides all of the characteristic views of the particle described in earlier studies [11,18] and these views of the particle are evident in class averages defined by computational analysis. Columns A, B and C of row 1 show class averages of negatively stained sample corresponding to the 'V' shape, the triangular and rectangular views, respectively. In row 2, class averages approximating mirror images of those in row 2 are presented, as expected for a suitable data set of images for three-dimensional reconstruction. Significantly, these views are also characteristic of image averages of frozen hydrated multisynthetase complex (row 3). Because images obtained by the two specimen preparation techniques are consistent, it is expected that both types can provide accurate reconstructions of the three-dimensional structure.

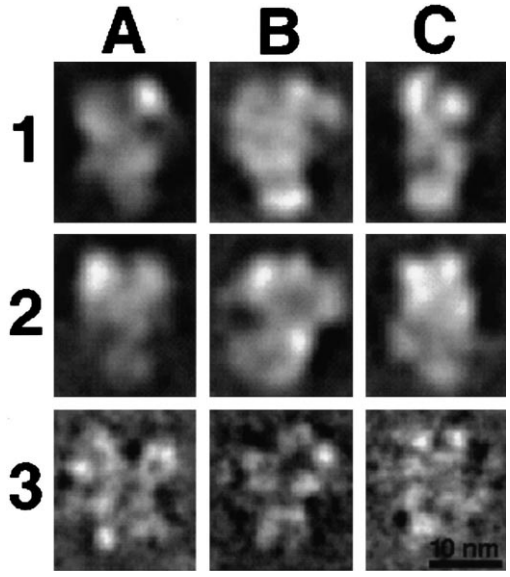

Fig. 1. Images of the multisynthetase complex in deep negative stain or vitreous ice correlate with previously observed characteristic views. Image averages show the three-domain view with a central cleft (column A), the triangular view (column B) and the rectangular view (column C). Row 1: Negatively stained sample with each average containing approximately 100 images. Row 2: Mirror image averages from those in row 1. Row 3: Frozen hydrated sample with each average containing approximately 50 images.

3.2. Three-dimensional architecture of the multisynthetase complex

Fig. 2 shows surface representations of three-dimensional volumes of the multisynthetase complex calculated from both negatively stained and frozen hydrated samples. Column A depicts results obtained by application of the random conical tilt method to negatively stained images. The volume has been filtered to its resolution limit of 30 Å. As a starting reference for description of other rotational views of the particle, the top image is termed the 'front' view. The subsequent selected rotations demonstrate the structural features of the particle.

The overall shape is an asymmetric triangle measuring 18.9 nm in height. The width is 16.2 nm at the top of the volume and narrows to 11.5 nm at the bottom. The difference in height of the 'arms' is 4.7 nm. Exceptionally striking is the 4 nm diameter deep central cleft which extends through two-thirds of the length of the volume. Rotation of the volume about its vertical or *y*-axis generates the left, back and right views. From these one can see that the thickness of the particle is 10 nm and that there are openings or indentations on most sides of the structure. The top and bottom views are generated by rotation of the front view around its horizontal or *x*-axis. The top view emphasizes the deep penetration of the cleft into the structure and the bottom view shows this end to be closed.

Column B presents the volume calculated from images of frozen hydrated sample. The reconstruction was obtained using angles derived from projection mapping using the negatively stained volume as a reference. The volume was filtered to its resolution limit of 36 Å. The data set contains only

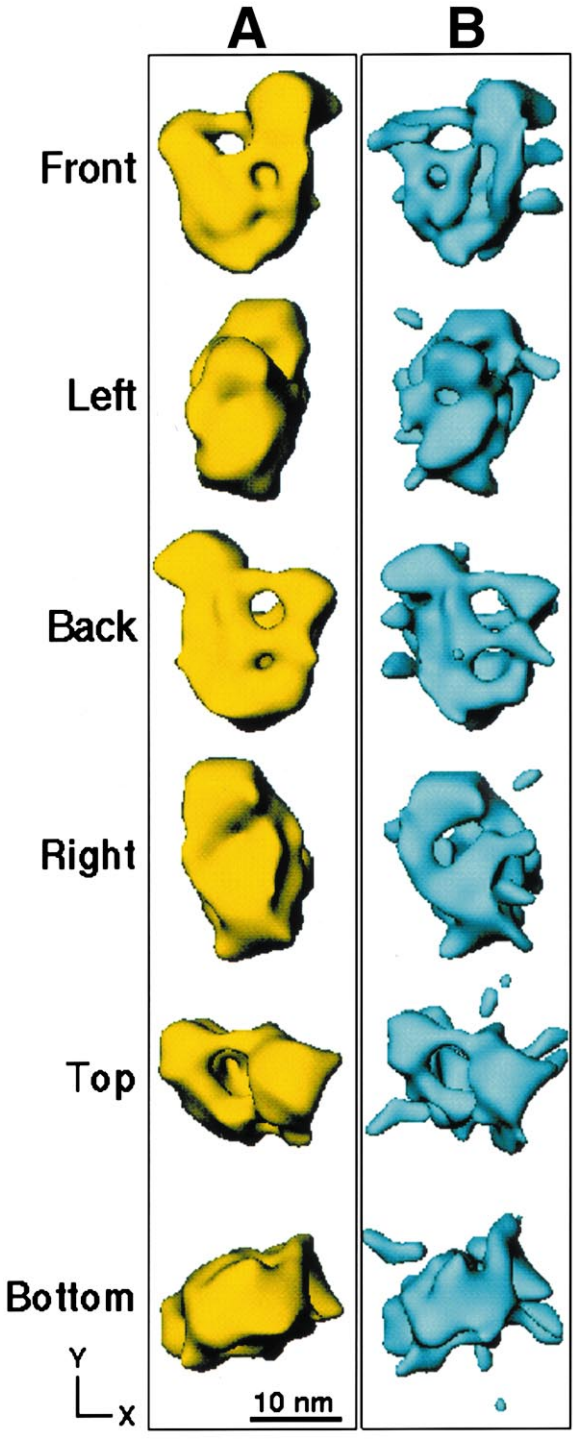

Fig. 2. Three-dimensional volumes of the multisynthetase complex derived from electron microscopic images in deep negative stain or vitreous ice are similar in all views. Column A depicts the volume calculated from 8233 images of negatively stained sample; column B depicts the volume calculated from 741 images of frozen hydrated sample. Resolution of the volumes is 30 and 36 Å, respectively. Starting with the front views, volumes are shown rotated in 90° increments around the *y* (vertical) axis giving left, back and right views or by 90° or 180° around the *x* (horizontal) axis giving top and bottom views.

about one-tenth the number of images as that for the negatively stained sample (741 versus 8233, respectively) due to difficulties in effective removal of the high glycerol concentration required for storage of the multisynthetase complex. Thus, there is correspondingly more noise in the volume as seen by the extra densities 'floating' around the particle. A much larger data set is needed to maximize resolution of the frozen hydrated structure. Nonetheless, it is clear that this initial ice volume reiterates the structural features of the multisynthetase complex visible in the volume derived from negatively stained images. Both volumes have the same dimensions and shape, the main protein densities are arranged in an asymmetric triangle, and a deep central cleft is present. Of particular importance is that the thickness of the two volumes in the side views (left or right) are the same, indicating that there is no artifactual flattening of the structure in the deep negative stain preparation method.

The accuracy of the negatively stained volume is further supported by the plot of coverage of Eulerian angles (Fig. 3) which shows that the volume contains images from essentially all of the angles. Moreover, there is no marked overrepresentation of particular views. Furthermore, projections of the volumes match actual image averages (Fig. 4). Three representative averages of negatively stained images are shown (row 1). These are reproduced by projections of the volume derived from this data set after rotation of the volume to the corresponding angles. This is depicted with the volume as surface representations in row 2 and in projections in row 3. Projections of the volume derived from images in ice (row 4) also show excellent correlation with the class averages of negatively stained images. These data provide additional evidence for the accuracy of the calculated volumes. However, in order to control for any possible bias introduced by alignment of the images in ice to the negatively stained volume, a third volume was calculated independently from any reference volume from a data set of images of frozen hydrated sample using an orientation search algorithm [17] to define the Eule-

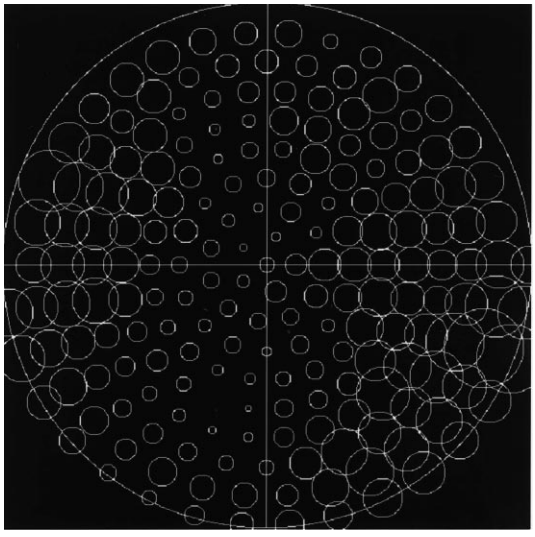

Fig. 3. Angular distribution of the images comprising the multisynthetase complex volume calculated from negatively stained images is essentially complete. A circle is present for each of the angular projections of the reference volume to which images were mapped. The diameter of the circle increases with the number of images corresponding to each projection.

rian angles among class averages. Projections of this volume at the appropriate angles (row 5) also match negatively stained image averages, as well as projections of the other two volumes.

The consistency of the volumes and their major structural features are further emphasized in Fig. 5, which depicts 'front' projections of the three-dimensional volumes of the multisynthetase complex determined in this study. The overall architecture is an asymmetric triangular arrangement of protein domains around a deep central cavity. Superposition of density contours (column B) emphasizes the distribution of major protein densities into two upper 'arms' and a 'base', as well as the lack of any density in the center of the structure.

4. Discussion

In this study, three-dimensional volumes of the multisynthetase complex have been calculated from images in negative stain and in vitreous ice. The structural characteristics are consistent regardless of specimen preparation method (negative stain or vitreous ice), angular assignment method (random conical tilt, projection mapping or orientation search), or size of the image data set. These results not only provide validity for the calculated volumes, but also suggest that studies of the particle in either deep negative stain or in vitreous ice will provide consistent and reliable information at resolutions in the range of 20–30 Å. Other studies of both asymmetric and symmetric protein complexes in which volumes calculated from frozen hydrated specimens were compared to those derived from negative staining with methylamine tungstate have also shown excellent agreement between volumes [19,20]. This study of the multisynthetase complex using uranyl acetate as the heavy metal stain adds an additional structure to the set of particles for which images in deep negative stain give three-dimensional reconstructions comparable to those obtained by cryoelectron microscopy [21].

The three-dimensional architecture of the multisynthetase complex is characterized by a triangular arrangement of major protein domains around a deep central cavity. This result is in good agreement with our working model which was derived from non-computational analysis of negatively stained electron micrographs [11], dissociation experiments [18] and cross-linking data [5]. This also provides a straightforward approach for comparison of descriptions of the internal organization of the multisynthetase complex that have been presented by different laboratories [7–9]. The stage is clearly set for refinement of the structure of the multisynthetase complex to high resolution and for precise localization of its constituent polypeptides.

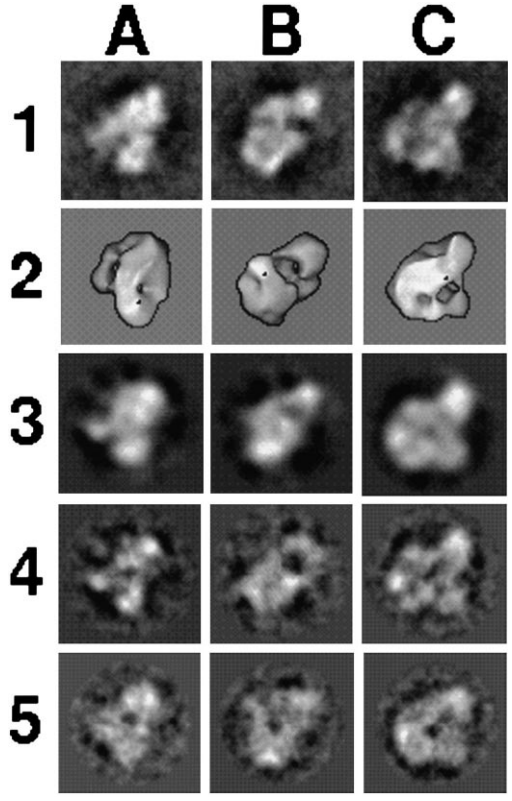

Fig. 4. Projections of the calculated volumes match averages of experimental images. Columns A–C: Selected views of the multisynthetase complex. Row 1: Averages of negatively stained images containing 93, 92 and 88 images, respectively. Row 2: Surface representations of the refined volume from negatively stained images oriented in the same view as the image averages. Row 3: Projections at comparable angles of the volume calculated from negatively stained images. Row 4: Projections at the same angles of the volume calculated by alignment of images of frozen hydrated sample to the negatively stained reference volume. Row 5: Projections at the same angles of the volume calculated from frozen hydrated images with angles determined by orientation search.

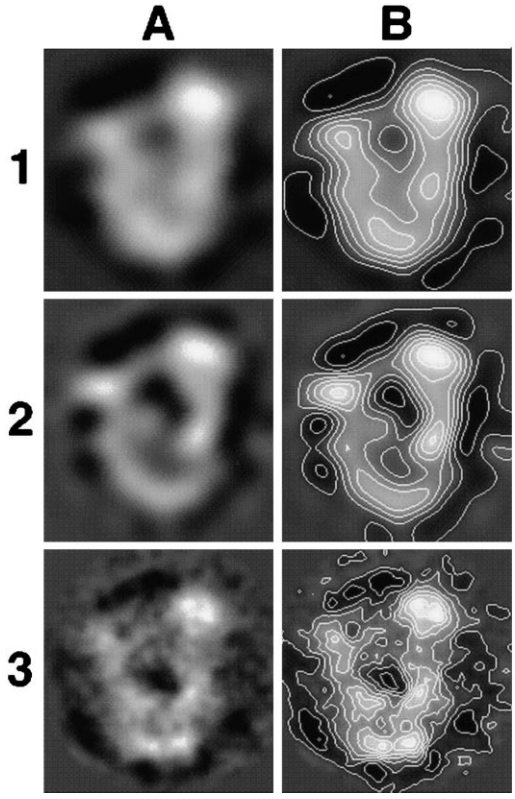

Fig. 5. Projections in the 'front' view of the three types of volumes all show an asymmetric triangular arrangement of high density domains and central cavity within the multisynthetase complex. Row 1: Negatively stained volume. Row 2: Ice volume obtained by alignment to the negatively stained reference. Row 3: Ice volume calculated by the angular search method. Projections are shown plain (column A) or with density contour overlays (column B). In each case, white areas are those of highest particle density and black areas of lowest density. Overlay lines show density level divisions.

The shape of the multisynthetase complex and the existence of its central cavity raise interesting questions regarding the function of the particle. For example, a mechanism that would require large tRNA substrates to enter the cavity in order to be aminoacylated appears unlikely given the rapidity of the protein biosynthesis process. However, the many cavities or 'windows' into the structure may allow access by the acceptor stem to a concentrated pool of amino acids. This type of compartmentalization was suggested by experiments measuring protein synthesis in permeabilized cells (reviewed in [22]). Current studies in this laboratory are exploring this question by examining the positioning of tRNAs on the multisynthetase complex.

It has long been suggested that the components of eukaryotic protein biosynthesis are highly organized into a 'supramolecular machine' (reviewed in [23]). Indeed, the multisynthetase complex described in this study is considered the 'core' of a much larger in vivo assembly of most, if not all, of these enzymes. Thus, another puzzle to be solved is how the 'core' multisynthetase complex fits into and functions within these structures. Full characterization of its structure, as begun by calculation of these initial three-dimensional volumes, is a prerequisite for investigations of its interaction with other aminoacyl-tRNA synthetases, protein synthesis factors, ribosomes and other cellular elements that act to organize protein biosynthesis.

Of significant interest is the localization of p43, the precursor form of EMAPII, at or near the center of the multisynthetase complex [7] bridging the three structural domains described in the working model of the particle. Now, with a solid three-dimensional reference volume in hand, we can define the structural role of this polypeptide and examine the seemingly incongruous association of an inflammatory cytokine with a central component of protein biosynthesis.

Acknowledgements: This work was supported by the National Science Foundation under Grant MCB-0090839 (M.T.N.) and by the CNRS under Grant PCV-2000 (N.B.). The excellent skills of Mr. Anthony Warrington in protein purification are gratefully acknowledged. Dr. J. David Dignam is thanked for helpful discussions and comments on the manuscript.

References

[1] Ibba, M. and Söll, D. (2000) Annu. Rev. Biochem. 69, 617–650.
[2] Martinis, S.A., Plateau, P., Cavarelli, J. and Florentz, C. (1999) Biochimie 81, 693–700.
[3] Quevillon, S., Agou, F., Robinson, J.C. and Mirande, M. (1997) J. Biol. Chem. 272, 32573–32579.
[4] Yang, D.C.H. (1996) Curr. Top. Cell Regul. 34, 101–136.
[5] Norcum, M.T. and Warrington, J.A. (1998) Protein Sci. 7, 79–87.
[6] Norcum, M.T. and Dignam, J.D. (1999) J. Biol. Chem. 274, 12205–12208.
[7] Norcum, M.T. and Warrington, J.A. (2000) J. Biol. Chem. 275, 17921–17924.
[8] Quevillon, S., Robinson, J.C., Berthonneau, E., Siatecka, M. and Mirande, M. (1999) J. Mol. Biol. 285, 183–195.
[9] Rho, S.B., Kim, M.J., Lee, J.S., Seol, W., Motegi, H., Kim, S. and Shiba, K. (1999) Proc. Natl. Acac. Sci. USA 96, 4488–4493.
[10] Nathanson, L. and Deutscher, M.P. (2000) J. Biol. Chem. 275, 31559–31562.
[11] Norcum, M.T. (1989) J. Biol. Chem. 264, 15043–15051.
[12] Cyrklaff, M., Roos, N., Gross, H. and Dubochet, J. (1994) J. Microsc. 175, 135–142.
[13] Dubochet, J., Adrian, M., Chang, J.J., Homo, J.C., Lepault, J., McDowall, A.W. and Schultz, P. (1988) Q. Rev. Biophys. 21, 129–228.
[14] Frank, J., Radermacher, M., Penczek, P., Zhu, J., Li, Y., Ladjadj, M. and Leith, A. (1996) J. Struct. Biol. 116, 190–199.
[15] Radermacher, M., Wagenknecht, T., Verschoor, A. and Frank, J. (1987) J. Microsc. 146, 113–136.
[16] Penczek, P., Radermacher, M. and Frank, J. (1992) Ultramicroscopy 40, 33–53.
[17] Penczek, P.A., Zhu, J. and Frank, J. (1996) Ultramicroscoppy 63, 205–218.
[18] Norcum, M.T. (1991) J. Biol. Chem. 266, 15398–15405.
[19] Kolodziej, S.J., Klueppelberg, H.U., Nolasco, N., Ehses, W., Strickland, D.K. and Stoops, J.K. (1998) J. Struct. Biol. 123, 124–133.
[20] Stoops, J.K., Baker, T.S., Schroeter, J.P., Kolodziej, S.J., Niu, X.D. and Reed, L.J. (1992) J. Biol. Chem. 267, 24769–24775.
[21] Harris, J.R. (1997) Negative Staining and Cryoelectron Microscopy: The Thin Film Techniques, BIOS Scientific, Oxford.
[22] Clegg, J.S. (1992) Curr. Top. Cell Regul. 33, 3–14.
[23] Kisselev, L.L. and Wolfson, A.D. (1994) Prog. Nucleic Acid Res. Mol. Biol. 48, 83–142.